

## Ligand Binding to the Hoogsteen–WC Groove of TAT Base Triplets: Thermodynamic Contribution of the Thymine Methyl Groups

Dionisios Rentzeperis<sup>†</sup> and Luis A. Marky\*

Department of Chemistry, New York University  
New York, New York 10003

Received November 16, 1994

The formation of triplexes, by the specificity of a third oligonucleotide strand to its cognate nucleic acid duplex through the formation of Hoogsteen hydrogen bonds, has been proposed as an approach to the control of gene expression, genome mapping, and therapeutic applications.<sup>1</sup> Therefore, it is of considerable importance to determine the overall physical–chemical properties of triplexes including structure, energetics, and interaction with small molecules.

In the formation of a pyrimidine–purine–pyrimidine triplex, the contribution of hydrophobic interactions has been illustrated by the observed increase in the thermodynamic stability of triplexes containing 5'-methyl cytosine in the third strand instead of cytosine<sup>2–4</sup> as well as in NMR results that indicated a structural hydration around these atomic groups.<sup>5</sup> The contribution of hydrophobic interactions should be more pronounced in the case of triplexes with exclusively dT\*dA\*dT base triplets, in which both thymine methyl groups are aligned in the same groove and exposed to the solvent (see Figure 1).

We used a combination of spectroscopic and high-sensitivity calorimetric techniques to investigate (i) the order–disorder transition of two DNA oligomers, d(A<sub>7</sub>C<sub>5</sub>T<sub>7</sub>C<sub>5</sub>T<sub>7</sub>) (triplex) and d(A<sub>3</sub>C<sub>5</sub>T<sub>7</sub>C<sub>5</sub>A<sub>4</sub>) (duplex), designed to form intramolecular double hairpins in the triplex<sup>6–8</sup> and duplex conformation that resemble the proposed and unusual structures that homopurine–homopyrimidine sequences may adopt *in vivo*,<sup>9</sup> and (ii) their interaction with the minor groove ligand netropsin. Each double hairpin melts in monophasic transitions with transition temperatures that are independent of strand concentration. The triplex transition enthalpies,  $\Delta H_{\text{cal}}$ , decreased with increasing salt concentration, yielding an apparent heat capacity effect that may be the result of removal of electrostricted water molecules and the formation at high salt concentration of a triplex structure with better defined grooves. Circular dichroism (CD) and isothermal titration calorimetry (ITC) titrations yielded netropsin–DNA stoichiometries of 2:1 (triplex) and 1:1 (duplex); binding of the first netropsin is accompanied by binding affinities,  $K_b$ , of  $\sim 10^5$  (triplex) and  $\sim 10^7$  (duplex) and low

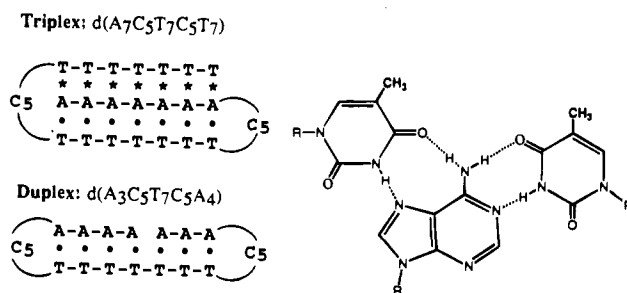


**Figure 1.** Sequences and schematics of hairpins. The structure of a T\*A•T base triplet, with the thymine methyl groups in boldface, is shown on the right.

binding heats,  $\Delta H_b$ , of  $-2$  and  $-6$  kcal/mol, respectively. However, the association of the second netropsin to the triplex is accompanied by a  $K_b$  of  $10^5$  and a high  $\Delta H_b$  of  $-12$  kcal/mol. Our combined thermodynamic results suggest the formation of a hydrophobic groove in this triplex by the spine of thymine methyl groups, that provides an additional binding site for the minor-groove ligand netropsin.

The oligomer sequences d(A<sub>7</sub>C<sub>5</sub>T<sub>7</sub>C<sub>5</sub>T<sub>7</sub>) and d(A<sub>4</sub>C<sub>5</sub>T<sub>7</sub>C<sub>5</sub>A<sub>3</sub>) were synthesized by phosphoramidite chemistry, purified by HPLC, and desalted on a Sephadex G-10 column. The order–disorder transition of each oligomer was characterized by following the changes in absorbance (ultraviolet (UV) melts) and excess heat capacity (differential scanning calorimetry (DSC) melts) as a function of temperature. Relative to the duplex, the triplex optical melt at 260 nm shows a 4% higher hypochromicity that corresponds to the additional stacking contribution of dA\*dT Hoogsteen base-pairs,<sup>10</sup> and its circular dichroism spectrum shows a 70% reduction in the molar ellipticity value at 220 nm, consistent with the formation of a triplex.<sup>11</sup>

Figure 2a shows typical DSC melting curves. For each double hairpin and in the range 0.02–1.1 M NaCl, we obtained melting curves that are monophasic with transition temperatures independent of strand concentration, confirming the exclusive formation of intramolecular species. This melting behavior is expected for the control duplex; however, for the triplex it indicates a simultaneous and coupled disruption of both Hoogsteen and Watson–Crick base-pair stacking interactions. Table 1 summarizes the thermodynamic results at 5 °C for the formation of each double hairpin; at each salt concentration their formation results from the characteristic partial enthalpy–entropy compensation. In 1.1 M NaCl, the  $\Delta H_{\text{cal}}$  for the triplex is 26.2 kcal more exothermic than that of the duplex and corresponds to the formation of Hoogsteen base pairing and extra base stacking interactions. If all seven base triplets are formed, then we estimate an average value of  $-3.7$  kcal/mol for the formation of a Hoogsteen dA\*dT base pair, in agreement with previously reported values ranging from  $-2.4$  to  $-3.7$  kcal/mol.<sup>11,12</sup> In addition, the triplex has a higher uptake of counterions (0.05 mol of Na<sup>+</sup>/(mol of P<sub>i</sub>)), consistent with its higher charge density. The most interesting observation is that the triplex  $\Delta H_{\text{cal}}$  becomes less favorable with an increase in salt concentration, contrary to what is commonly observed in DNA duplexes containing exclusively dA•dT base pairs.<sup>11,13</sup> This effect indirectly yields an apparent heat capacity,  $\Delta C_p$ , of  $+680$  cal K<sup>-1</sup>/(mol of triplex) and suggests that there is further exposure of hydrophobic groups at the higher salt concentration.

(10) Pilch, D. S.; Brousseau, R.; Shafer, R. H. *Nucleic Acids Res.* **1990**, *18*, 5743.

(11) Hopkins, H. P.; Hamilton, D. D.; Wilson, W. D.; Zon, G. J. *Phys. Chem.* **1993**, *97*, 6555.

(12) Park, Y. W.; Breslauer, K. J. *Proc. Natl. Acad. Sci. U.S.A.* **1992**, *89*, 6653.

(13) Rentzeperis, D.; Rippe, K.; Jovin, T. M.; Marky, L. A. *J. Am. Chem. Soc.* **1992**, *114*, 5926.

\* Author to whom correspondence should be addressed.

<sup>†</sup> Present address: Department of Biology, Massachusetts Institute of Technology, 77 Massachusetts Ave., Boston, MA 02139.

(1) Cooney, M.; Czernuszewicz, G.; Postel, E. H.; Flint, S. J.; Hogan, M. E. *Science* **1988**, *241*, 456. Felsenfeld, G.; Davies, D.; Rich, A. *J. Am. Chem. Soc.* **1957**, *79*, 2023. Grigoriev, M.; Preseuth, D.; Robin, P.; Hemar, A.; Saison-Behmoras, T.; Dautry-Varsat, A.; Thuong, N. T.; Hélène, C.; Harel-Bellan, A. *J. Biol. Chem.* **1992**, *267*, 3389. Le Doan, T.; Perrouault, L.; Praseuth, D.; Habboub, N.; Decout, J. L.; Thuong, N. T.; Lhomme, J.; Hélène, C. *Nucleic Acids Res.* **1987**, *15*, 7749. Maher, L. J.; Dervan, P. B.; Wold, B. *Biochemistry* **1990**, *29*, 8820; **1992**, *31*, 70. Morgan, A. R.; Wells, R. D. *J. Mol. Biol.* **1968**, *37*, 63. Moser, H. E.; Dervan, P. B. *Science* **1987**, *238*, 645. Wang, S.; Kool, E. T. *Nucleic Acids Res.* **1994**, *22*, 2326.

(2) Lee, J. S.; Woodsworth, M. L.; Latimer, L. J. P.; Morgan, A. R. *Nucleic Acids Res.* **1984**, *12*, 6603.

(3) Povsic, T. J.; Dervan, P. B. *J. Am. Chem. Soc.* **1989**, *111*, 3059.

(4) Xodo, L. E.; Manzini, G.; Quadrioglio, F.; van der Marel, G. A.; van Boom, J. H. *Nucleic Acids Res.* **1991**, *19*, 5625.

(5) Radhakrishnan, I.; Patel, D. J. *Biochemistry* **1994**, *33*, 11405. *Curr. Opin. Struc. Biol.* **1994**, *2*, 395.

(6) Häner, R.; Dervan, P. B. *Biochemistry* **1990**, *29*, 9761.

(7) Sklenár, V.; Feigon, J. *Nature (London)* **1990**, *345*, 836.

(8) Radhakrishnan, I.; de los Santos, C.; Patel, D. J. *J. Mol. Biol.* **1991**, *221*, 1403.

(9) Mirkin, S. M.; Lyamichev, V. I.; Drushlyak, K. N.; Dobrynin, V. N.; Filippov, S. A.; Frank-Kamenetskii, M. D. *Nature* **1987**, *330*, 495.

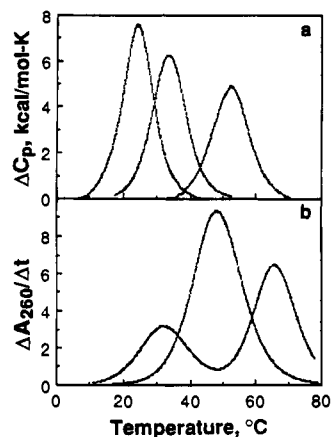


**Figure 2.** (a) DSC curves of 0.15 mM triplex, measured with a Microcal MC-2 calorimeter (Northampton, MA), in 10 mM NaP<sub>i</sub> buffer, 0.1 mM Na<sub>2</sub>EDTA at pH 7.0 and NaCl concentration (from left to right) of 16 mM, 0.11 M, and 1.1 M. Analysis of these curves, using procedures reported previously,<sup>13,14</sup> yielded  $T_m$ 's and standard thermodynamic profiles for the helix-coil transition of each oligomer. (b) UV differential melting curves: monophasic curve (free triplex) and biphasic curve (2:1 netropsin-triplex complex), measured at 260 nm and a heating rate of 1.0 °C/min with a thermoelectrically controlled Perkin-Elmer 552 spectrophotometer and interfaced to a PC-XT computer for data acquisition, in the same buffer at 0.6 M NaCl and oligomer concentration of 2.4  $\mu$ M in strands.

**Table 1.** Thermodynamic Profiles for the Formation of Double Hairpins at 5 °C<sup>a</sup>

[NaCl] mM	$T_m$ (°C)	$\Delta G^\circ_{\text{cal}}$ (kcal/mol)	$\Delta H_{\text{cal}}$ (kcal/mol)	$T\Delta S_{\text{cal}}$ (kcal/mol)	$dT_m/d \log$ [Na <sup>+</sup> ] (K)	$\Delta n_{\text{Na}^+}$ (mol of Na <sup>+</sup> /mol)
Triplex						
16	24.5	-6.0	-92.0	-86.0	13.8	3.38
107	33.3	-7.5	-80.9	-73.8	13.8	3.19
1100	52.4	-10.5	-71.9	-61.4	19.3	2.81
Duplex						
1100	35.9	-4.6	-45.7	-41.1	11.8	0.97

<sup>a</sup> The  $T_m$ 's are within  $\pm 0.5$  °C, and  $\Delta G^\circ$  values are within 5%;  $\Delta H$  ( $\pm 3\%$ ),  $T\Delta S$  ( $\pm 8\%$ ), and  $\Delta n_{\text{Na}^+}$  ( $\pm 5.0\%$ ). The uptake of counterions,  $\Delta n_{\text{Na}^+}$ , was calculated from the equation:  $dT_m/d \ln [\text{Na}^+] = 0.9(RT_m^2/\Delta H_{\text{cal}})\Delta n_{\text{Na}^+}$ .<sup>13,14</sup>

Furthermore, as the increase in salt concentration shifts the triplex transition to higher temperatures, there is partial compensation of the unfavorable enthalpy difference with a favorable differential entropy and a marginal differential counterion uptake ( $-0.6$  mol of Na<sup>+</sup>/(mol of triplex)). Such compensation is characteristic of processes where changes in the overall hydration state take place.<sup>14,15</sup> If we assume similar random coil states, then at low salt concentration, the triplex structure must be stabilized additionally by immobilization of electrostricted water molecules. The increase in salt concentration would tend to reduce the repulsive electrostatic interactions by screening of the negatively charged phosphate groups, yielding a net reduction of the electrostriction of water molecules and optimizing base-pair stacking and hydrogen-bonding interactions. At high salt concentration, the triplex structure has better defined grooves such as the hydrophobic spine of thymine methyl groups in the Hoogsteen-Watson groove of the triplex.<sup>5</sup> In this salt range, we estimate a removal of  $\sim 82$  electrostricted water molecules per triplex from the positive differential compensation of 24.6 kcal/mol.<sup>16,17</sup>

(14) Zieba, K.; Chu, T.; Kupke, D. W.; Marky, L. A. *Biopolymers* **1993**, *33*, 117.

(15) Rentzperis, D.; Kupke, D. W.; Marky, L. A. *J. Phys. Chem.* **1992**, *96*, 9612.

(16) Gasan, A. I.; Maleev, V. Ya.; Semenov, M. A. *Stud. Biophys.* **1990**, *136*, 171.

We used the interaction of the minor groove ligand netropsin, which binds to DNA in the "B" conformation with high specificity for dA·dT base pairs<sup>18,19</sup> to probe the triplex grooves thermodynamically. The netropsin interaction to each double hairpin is investigated by using CD spectroscopy, melting, and ITC techniques. CD show stoichiometries of 2:1 for the netropsin-triplex complex and 1:1 for the netropsin-duplex complex. The binding of the second netropsin is accompanied by only a 15% change in the induced CD signal of the first ligand, indicating binding of the ligand to a different environment.

The UV melt of the 2:1 netropsin-triplex complex is biphasic (Figure 2b). The first transition has a lower  $T_m$  than that of the unligated triplex, while the second transition has a higher  $T_m$ . The first transition corresponds to the melting of the 2:1 netropsin-triplex to 1:1 netropsin-duplex accompanied by the dissociation of 1 equiv of netropsin, and the second transition to melting of the 1:1 netropsin-duplex complex (with a dangling end) to the coil state with the dissociation of the second equivalent of netropsin. Therefore, netropsin binding thermodynamically destabilizes the formation of the triplex, and this ligand is recognizing a second groove of the triplex.

To determine the nature of the destabilization of the triplex domain upon netropsin binding, we performed isothermal calorimetric titrations at 5 °C.<sup>20,21</sup> The fits of the ITC binding isotherms show the following (i) complex stoichiometries similar to the ones obtained in CD titrations; since the netropsin binding site for this type of triplex spans seven dA·dT base pairs<sup>12</sup> and the duplex is binding only one netropsin molecule (i.e., the loops are not binding any at all), then the second netropsin is binding in a different groove of the triplex; (ii) that binding of the first netropsin to the triplex, relative to the control duplex, results in a  $K_b$  that is 2 orders of magnitude smaller and a less exothermic heat; therefore, netropsin binds better to the minor groove of the duplex, suggesting that the triplex has a narrower minor groove; (iii) that the  $\Delta H_b$  for the second netropsin to the triplex is far more exothermic, as expected for the binding of netropsin to a hydrophobic groove in which the complex is stabilized primarily by van der Waals interactions. In addition, the enthalpic contribution for releasing hydrophobic or structural water from a dA·dT environment has been estimated to be exothermic,<sup>14</sup> and since we measured a heat capacity effect with this triplex, we conclude that the likely binding site of the second netropsin is the hydrophobic spine of thymine methyl groups in the Hoogsteen-Watson groove of the triplex. This additional site is reported here for the first time.<sup>12,22</sup>

**Acknowledgment.** This research was supported by Grant GM-42223 from the National Institutes of Health and BRSG Grant 2 S07 RR 07062 C-26, awarded by the Biomedical Research Support Grant Program, Division of Research Resources, NIH.

**Supplementary Material Available:** Figure of CD and ITC titrations and table of the thermodynamic profiles for netropsin binding (2 pages). This material is contained in many libraries on microfiche, immediately follows this article in the microfilm version of the journal, can be ordered from the ACS, and can be downloaded from the Internet; see any current masthead page for ordering information and Internet access instructions.

JA943714G

(17) Tunis, M.-J. B.; Hearst, J. E. *Biopolymers* **1968**, *6*, 1325.

(18) Zimmer, C.; Wahnert, U. *Prog. Biophys. Mol. Biol.* **1986**, *47*, 31.

(19) Marky, L. A.; Kupke, D. W. *Biochemistry* **1989**, *28*, 9982.

(20) Wiseman, T.; Williston, S.; Brandts, J. F.; Lin, L.-N. *Anal. Biochem.* **1989**, *179*, 131.

(21) Lin, L.-N.; Mason, A. B.; Woodworth, R. C.; Brandts, J. F. *Biochemistry* **1991**, *30*, 11660.

(22) Durand, M.; Thuong, N. T.; Maurizot, J. C. *J. Biol. Chem.* **1992**, *267*, 24394.